Ultrasonic Imaging of Propagation of Electric Excitation in Heart Wall

Hiroshi Kanai
Dept. of Electronic Engineering
Graduate School of Engineering, Tohoku University
Sendai 980-8579, Japan
E-mail: kanai@ecei.tohoku.ac.jp

Abstract— **We have already shown that the pulsive vibration is excited on the myocardium 15 ms after the electrical stimulation to an isolated heart [1]. If the heart wall vibration caused by spontaneous electric excitation is visualized using ultrasound, the regional cell damage regarding electric potential due to diseases can be noninvasively detected. In this study, the spatial distribution of the minute vibration caused just around R-wave of ECG is visualized in *in vivo* experiments as follows: By the ultrasonic measurement of the myocardial motion [2], we detect pulsive waves spontaneously caused by electrical excitation or valve closure. Using a sparse sector scan [3], the waves are measured almost simultaneously at about 1,000 points set in the heart wall at a high frame rate (400 Hz). The consecutive spatial distributions of the interpolated phase of the waves reveal wave propagation along the wall. The propagation time is several ms, which is too short to be detected by conventional methods. The method was applied to 5 healthy subjects. The spontaneously driven pulsive waves and their propagations were clearly visible in all subjects in the longitudinal-axis, short-axis, and apical views. Just after the Q-wave of ECG, the propagation started from the apex, which is close to the papillary muscle (terminal of Purkinje fiber), to the base side of the heart. Its propagation speed was slow (1-2 m/s for 20-100 Hz), which shows the propagation of electrical excitation. Then, after R-wave of ECG, another pulsive wave started to propagate reversely from base to apex. Since its speed was several m/s for about 50 Hz but there was dispersion, this is the shear wave caused by the mitral-valve closure. The method noninvasively reveals the propagation of electrical conduction wave by measuring regional myocardial response to it in human heart, which will be a novel tissue characterization of the heart.**

Keywords- electric excitation; pulsive waves; heart sounds; phased tracking method

I. INTRODUCTION

Though electrocardiography (ECG) has become an invaluable clinical tool for diagnosis of a broad range of cardiac conditions, the regional properties of the myocardium still cannot be directly measured. If the propagation of the spontaneous electric excitation in the heart wall is visualized, the regional cell damage regarding the electric potential due to diseases can be transthoracically detected.

We have already found that the pulsive vibration is caused on the extracted myocardium in response to the electrical stimulation [1]. The amplitude is minute of about 30 μm in displacement and 0.5 m/s in velocity and the delay of the response is about 15 ms. In this paper, this phenomenon is detected for the healthy human heart *in vivo* from chest wall by the simultaneous detection of the vibrations at about 1,000 points in the myocardium using ultrasound.

Though magnetic resonant imaging (MRI), computer tomography (CT), and conventional echocardiography enable clinical visualization of cross-sectional images of the human heart, the imaging is restricted to static configuration or the large motion (> 1 mm) with low frequency components (< 30 Hz). In the MRI, the time resolution is limited by the relaxation time (< 20 ms) of the tissue to the magnetic excitation. In conventional echocardiography, the detectable amplitude is still greater than the wavelength, which is equal to 410 μm for ultrasound with a frequency of 3.75 MHz. The tissue Doppler imaging technique [4-5] enables us to acquire motion distribution of the myocardium. By applying these methods to the detection of the displacement of the regional myocardium, the large show motion, that is, the contraction and relaxation of the regional myocardium, during one cardiac cycle is quantitatively detected using ultrasound-based method [6] and MRI [7]. However, the time resolution in the measured motion of the heart wall is very low (at most 16 ms). All these clinical imaging methodologies, therefore, cannot detect minute vibrations of the myocardium caused by the electrical excitation and cannot visualize their dynamic property.

We have developed a novel ultrasonic method to measure spatial distribution of the minute vibrations in the heart wall with high temporal resolution of 2 ms [8-10]. The detectable lower limits of the displacement and velocity are 0.2 μm and 0.1 mm/s, respectively, and the high frequency components until 100 Hz are detected. The measurement is almost simultaneously applied to about 1,000 points set in the heart wall region [2]. The spatial distribution regarding the instantaneous waveform or its phase of the specific frequency component is shown at every 2 ms, revealing the propagation of the vibration wave on the ultrasonic cross-sectional image of the heart wall [3]. We already found for healthy human subjects that some impulsive vibrations are mechanically caused by the closure of the heart valves [11] and they propagate along the heart wall with frequency dispersion [3], which agrees with the theoretical characteristics of the Lamb wave, a kind of the shear wave. In this paper, this novel method is applied to reveal the propagation of the electrical

conduction wave. Similar results were obtained in [12], in which high frame rate (8000 PRF) acquisition is employed for small animals with depth of about 10 mm. For human heart, however, this high frame rate cannot be realized. These new insights open the way for noninvasive analysis of the myocardium cell damage due to heart failure.

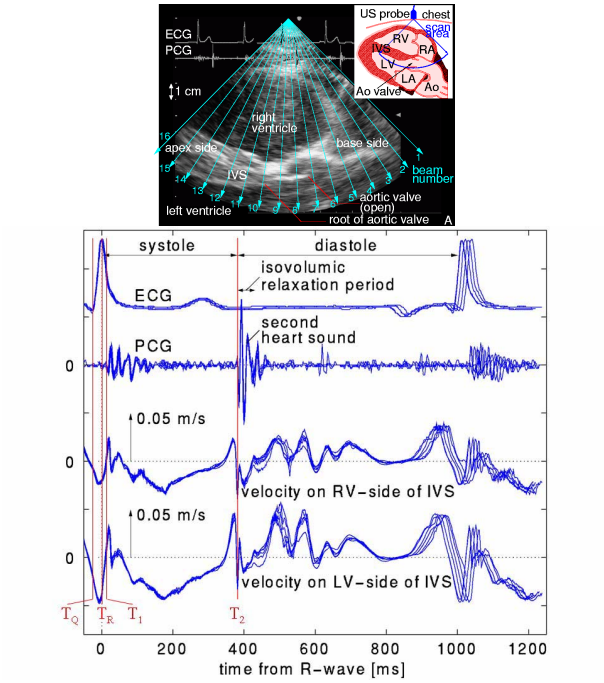

Figure 1. **upper:** A parasternal longitudinal-axis cross-sectional image measured by conventional ultrasound diagnosis system for a young healthy male. The upper-right inset shows the scanning range of the ultrasonic beams in this imaging. **lower**: Vibration waveforms on the heart wall observed *in vivo* for the healthy man. The observed two points are set at both side of the septum along the 13th ultrasonic beam. Each waveform for six consecutive cardiac cycles is overlaid. The times T_R, T_1, and T_2 respectively show the R-wave of the electrocardiogram, the beginning of the first heart sound, and the beginning of the second heart sound.

II. Distribution Of The Heart Wall Vibrations

Figure 1(upper) shows a typical cross-sectional image of a heart obtained by conventional echocardiography for a young healthy subject from the transthoracic parasternal longitudinal-axis view. The upper-right illustration shows the scanning range of the ultrasonic beams in this imaging. The large slow motion during one heartbeat is indeed recognized. Previously, to measure the original vibrations of the heart sounds, which are audible by stethoscope, we have developed an ultrasound-based transthoracic method to measure the minute vibrations at the points set in the heart wall as waveforms [8-10]. For this accurate measurement, the phase shift due to the myocardium during the short period (2 ms) of the succeedingly detected ultrasounds is detected with accuracy of 0.4 degrees by the newly developed method [8-9] and the time resolution is improved from about 16 ms in conventional echocardiography to about 2 ms. To realize this, the number of the transmitted directions of the ultrasonic beams is decreased from 240 to 16 as shown in blue arrows of Fig. 1(upper). For all of the multiple points preset at 75-μm intervals in the heart wall along the 16 ultrasonic beams, the minute vibrations in the heart wall are almost simultaneously measured as a waveform with a sampling interval of about 2 ms for the first time [8-9].

Figure 1(lower) shows a typical example of the vibration waveforms on both sides of the interventricular septum (IVS). Though 6 consecutive heartbeats are overlaid, we find the phenomena that there are minute rapid vibrations with high reproducibility among succeeding cardiac cycles, although these dynamic properties cannot be observed by any other conventional equipment (CT, MRI, conventional echocardiography). As shown by these waves, some discriminative impulses can be observed, especially at the beginning (T_1) of the first heart sound and at the beginning (T_2) of the second heart sound. Moreover, just before R-wave (T_R) of ECG, there is a pulsive vibration in Fig. 1(lower). Steepest pulse in these three distinctive vibrations is the mechanical vibrations caused by the closure of the semilunar valves (the aortic valve and pulmonary valve) at a time T_2 [11]. The pulsive vibration at a time T_1 is also a mechanically caused vibration due to the closure of the atrioventricular valves (the mitral valve and the tricuspid valve). These two waves at T_1 and T_2 are original vibrations of the two major heart sounds which can be audible using stethoscope. However, at a time T_R, there is not a possibility of the mechanically caused vibration because the atrioventricular valves are still open. By referring to [1], this vibration at T_R corresponds to the response of the myocardium to the electrical stimulation.

III. Propagation Of The Impulse Along The Wall

Since the wavelength of the detected impulsive wave is about 10 cm for a 30 Hz component and is comparable to that of the heart wall, its propagation phenomenon cannot be easily visualized by showing the amplitude distribution of the impulsive wave along the heart wall. Instead, the phase value of the impulsive wave, which varies from 0 to 360 degrees in one wavelength, is effective. Therefore, the phase values of the measured wave for a frequency component selected from 10 Hz to 100 Hz are color-coded for imaging of 2-D spatial distribution [2]. For this imaging, after the wave observed at each point preset in the heart wall is multiplied by the Hanning window with a short time of 35 ms, the short-time Fourier transform is applied to the resultant wave. By this procedure, the detected phase corresponds to the delay time of the specific frequency component to the center of the short time window. In this study, since the wavelength of the detected wave is far longer that the beam interval, the phase distribution is interpolated among the ultrasonic beams sparsely scanned in 16 directions so that the regional phenomena regarding the propagation of the wave can be clearly visualized. The phase delay from 0 to 2π radian is color coded as shown in the upper circle in Fig. 2 and displayed in the cross-sectional image. When there is a positive pulse just at the center of the window, the phase delay is zero and the employed color is "red". On the other hand, the negative pulse at the center (phase delay of π radian) corresponds to the color "cyan". For example, for the frequency component with f_0=60 Hz, π radian in the phase delay corresponds to the time delay of 8.3 ms ($=+\pi/2\pi\ f_0$). Moreover, from these consecutively observed cross-sectional 2-D images at every 2 ms, a motion picture is obtained.

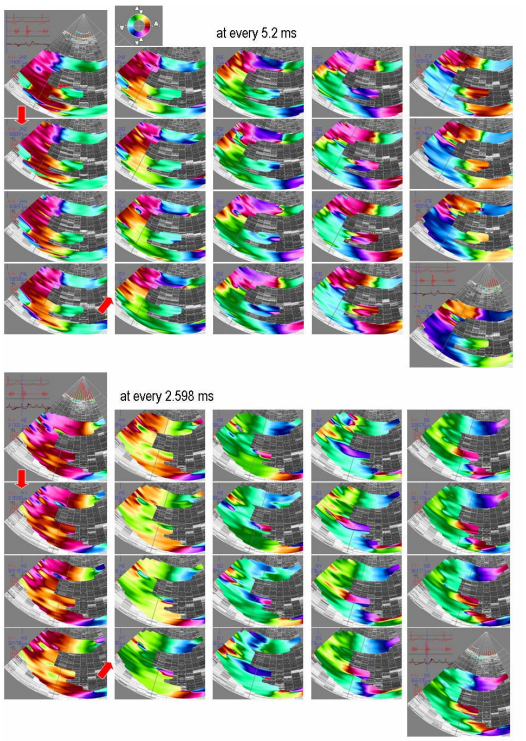

Figure 2. For a parasternal *longitudinal-axis cross-sectionalapproach* of a young healthy male, the resultant consecutive spatial distributions of color-coded phase values for 47 Hz component of the observed wavelets. **upper:** From T_R-177 ms to T_R-78 ms before the R-wave. **lower:** From T_2-7.8 ms to T_2+41.6 ms around the beginning of the second heart sound.

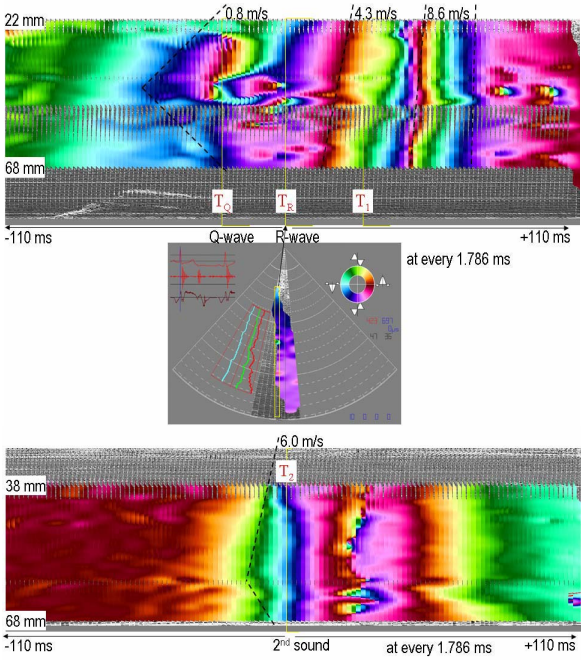

Figure 3. For a*n apical approach* of a young healthy male, the resultant consecutive spatial distributions of color-coded phase values for 47 Hz component of the observed wavelets. **upper:** From T_R-110 ms to T_R+110 ms around the R-wave. **lower**: From T_2-110 ms to T_2+110 ms around the beginning of the second heart sound.

IV. *In Vivo* Experimental Results

The method was applied to some healthy subjects. The spontaneously occurred pulsive waves and their propagations were clearly visible in all subjects in each consecutive phase distribution of the parasternal longitudinal-axis view (Fig. 2), and the apical view (Fig. 3), and the parasternal short-axis view (Fig. 4). Each of these figures shows the instantaneous phase distributions of specific frequency components involved in the vibrations simultaneously observed at about 1,000 points preset in the heart wall.

As shown in the consecutively observed figures (Figs. 2(upper) and 3(upper)), just before the Q-wave of ECG, the propagation started from the root of the papillary muscle, which is close to the terminal of Purkinje fiber, to the base side of the heart along the IVS. Since its propagation speed was slow (about 1 m/s) as in the previously published data for the extracted myocardium and there was no dispersion, these phenomena correspond to the response of the myocardium to the excitation due to the propagating electrical conduction wave.

At a time (T_1) 40 ms after R-wave of ECG, then, another pulsive waves start to propagate reversely from base to apex as clearly shown in Fig. 3(upper). There are two components with propagation speed of about 4 m/s and 8 m/s for 47 Hz, and there is large dispersion. Thus, this is the shear wave mechanically caused by the closure of the atrioventricular valves. The propagation time due to the both propagations of the vibrations is several milliseconds, which has not been recognized at all by any conventional techniques.

On the other hand, as shown in both of Figs. 2(lower) and 3(lower), just at the beginning (T_2) of the second heart sound, a few impulses are radiated from the root of aortic valve and propagates along the septum from the root to apical side of the heart. Its speed is about 6 m/s for 47 Hz and there is large dispersion. Thus, this is the shear wave mechanically caused by the closure of the semilunar valves.

In the observations, each vibration has the direction component along each ultrasonic beam. That is, in the parasternal longitudinal-axis view of Fig. 2, both directions of each ultrasonic beam and the detected vibration components are almost perpendicular to the septum. These vibrations propagate along the septum, that is, the propagation direction is almost perpendicular to the direction of the detected vibration, which means the shear component. On the other hand, in Fig. 3, both directions of each ultrasonic beam and the detected vibration components are almost perpendicular to the septum and the propagation direction is almost similar to the direction of the detected vibration, which means the longitudinal component. Since these mechanically excited two components have the similar propagation speeds of several m/s, this phenomenon is explained by a Lamb wave in a thin wall (the septum).

In the short-axis view of Fig. 4, each 2-D distribution is transformed from the circular shape in *x*-*y* coordinate system to the rectangular shape in *r*-θ coordinate system so that the propagation in circumferential direction can be easily identified as illustrated in Fig. 4. As shown in the consecutively observed

figures (Fig. 4(upper)), just after the Q-wave of ECG, the propagation started from the root of the papillary muscle, which is close to the terminal of Purkinje fiber, to the base side of the heart in clockwise direction when *x-y* plane is viewed from the foot of the subject. Since its propagation speed was slow (about 1 m/s for 20-100 Hz) and there was no dispersion, these phenomena correspond to the response of the myocardium to the excitation due to the propagating electrical conduction wave.

Then, at a time (T_1) 15 ms after R-wave of ECG, another pulsive wave started to propagate also in counterclockwise direction. Its speed was about 3 m/s for 22 Hz. Also as shown in Fig. 4(lower), just at the beginning (T_2) of the second heart sound, a few impulses are radiated from the point close to the root of aortic valve and propagates along the wall to the posterior wall also in counterclockwise direction. Since its speed was about 5 m/s for 37 Hz. These waves at T_1 and T_2 are the shear waves mechanically caused by the closure of the atrioventricular valves and semilunar valves, respectively.

V. Conclusions

To conclude, by observing rapid and minute vibration components simultaneously at about 1,000 points in the human heart wall to visualize the wave propagation along the heart wall, we found that there are three kinds of vibration propagation at T_R, T_1, and T_2 for the first time in human heart. By considering the cause, the time, and dispersion properties of each vibration, the vibration at T_R corresponds to response of the myocardium to the electrical conduction wave, which propagates from the root of the papillary muscle to the whole heart, and the vibration at T_1 and T_2 correspond to the propagation of the mechanically excited waves. Since each of these propagations depends on the regional myocardial characteristics, cell damage to the electrical excitation and viscoelasticity [2], respectively, these natural phenomena observed for the healthy human subjects and unified in this paper show a potential of the emerging motivation in noninvasive assessment of myocardium in the heart wall.

References

[1] H.Kanai, S.Katsumata, H.Honda, and Y.Koiwa, "Measurement and analysis of vibration in the myocardium telescopic motion for novel echo-graphic diagnosis," Acoustical Science and Technology, vol. 24, pp. 17-22, 2003.

[2] H. Kanai, "Propagetion of Spontaneously actuated pulsive vibration in human heart wall and *in vivo* viscoelasticity estimation," IEEE Trans UFFC, vol. 51, pp. 1931-1942, 2005.

[3] H.Kanai, S.Yonechi, I.Susukida, Y.Koiwa, H.Kamada, and M.Tanaka, "Onset of pulsatile waves in the heart walls at end-systole," Ultrasonics, vol. 38, pp. 405-411, 2000.

[4] G.R. Sutherland, M.J. Stewart, K.W.E. Groundstroem, C.M.Moran, A.Fleming, F.J.Guell-Peris, R.A.Riemersma, L.N.Fenn, K.A.A.Fox, and W.N.McDicken, "Color Doppler myocardial imaging: A new technique for the assessment of myocardial function," J. Amer. Soc. Echocardiogr., vol. 7, pp. 441–458, 1994.

[5] G.R.Sutherland, G.D.Salvo, P.Claus, J.D'hooge, and B.Bijnens, "Strain and strain rate imaging: A new clinical approach to quantifying regional myocardial function," J. Amer. Soc. Echocardiogr., vol. 17, no. 7, pp. 788–802, 2004.

[6] Y.Notomi, R.M.Setser, T.Shiota, M.G.Martin-Miklovic, J.A.Weaver, Z.B.Popovic, H.Yamada, N.L.Greenberg, R.D.White, and J.D.Thomas, "Assessment of left ventricular torsional deformation by doppler tissue imaging: validation study with tagged magnetic resonance imaging," Circulation, vol. 111, pp. 1141-1147, 2005.

[7] S.-J.Dong, P.S.Hees, C.O.Siu, J.L.Weiss, and E.P.Shapiro, "MRI assessment of LV relaxation by untwisting rate: a new isovolumic phase measure of τ," Am J Physiol Heart Circ Physiol, vol. 281, pp. H2002-H2009, 2001.

[8] H.Kanai, M.Sato, Y.Koiwa, and N.Chubachi, "Transcutaneous measurement and spectrum analysis of heart wall vibrations," IEEE Trans. UFFC, vol. 43, pp. 791-810, 1996.

[9] H.Kanai, H.Hasegawa, N.Chubachi, Y.Koiwa, and M.Tanaka, "Noninvasive evaluation of local myocardial thickening and its color-coded imaging," IEEE Trans. UFFC, vol. 44, pp. 752-768, 1997.

[10] H.Kanai, Y.Koiwa, and J.Zhang, "Real-time measurements of local myocardium motion and arterial wall thickening," IEEE Trans. UFFC, vol. 46, pp. 1229-1241, 1999.

[11] H.Kanai, and Y.Koiwa, "Myocardial rapid velocity distribution," Ultrasound Med. Biol. vol. 27, pp. 481-498, 2001.

[12] M.Pernot, K.Fujikura, S.D.Fung-kee-fung, and E.E.Konofagou, "Ecg-gated, mechanical and electromechanical wave imaging of cardiovascular tissues *in vivo*," Ultrasound Med. Biol. vol. 33, pp. 1075-1085, 2007.

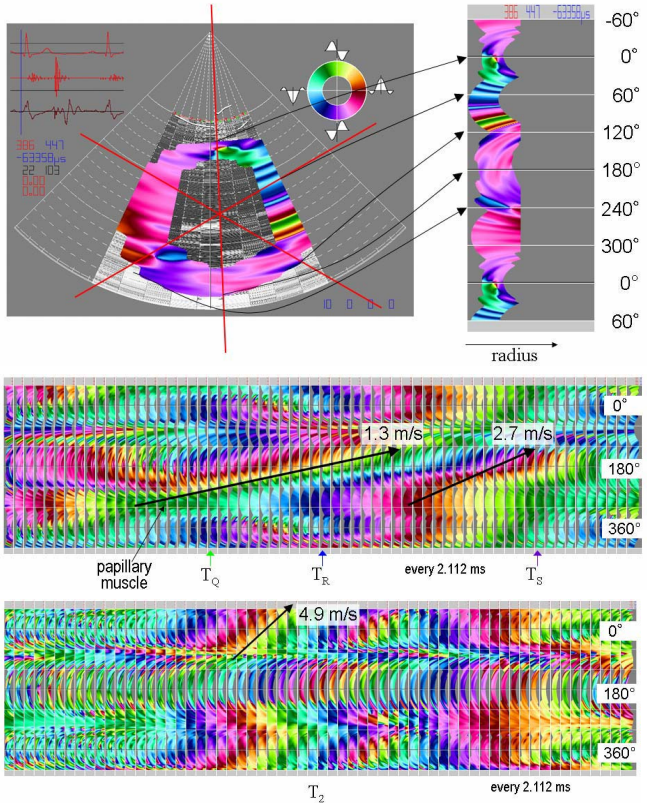

Figure 4. For a parasternal *short-axis cross-sectional apporach* of a young healthy male, the short-axis cross-sectional image in *x-y* plane is converted to *r*-θ plane as shown in the **upper** figure and the resultant consecutive spatial distributions in *r*-θ plane of color-coded phase values shown for 22 Hz component of the observed wavelets. **middle**: From T_R-63 ms to T_R+63 ms around the R-wave (22 Hz). **lower**: From T_2-63 ms to T_2+63 ms around the beginning of the second heart sound (37 Hz).